



Published in final edited form as:

*ChemBiochem*. 2009 May 25; 10(8): 1385–1391. doi:10.1002/cbic.200900092.

## Probing the Role of Backbone Hydrogen Bonding in a Critical $\beta$ -sheet of the Extracellular Domain of a Cys-loop Receptor

Kristin R. Gleitsman<sup>a</sup>, Henry A. Lester<sup>b</sup>, and Dennis A. Dougherty<sup>a,\*</sup>

<sup>a</sup>Division of Chemistry and Chemical Engineering, California Institute of Technology, 1200 E California Blvd, Pasadena, CA 91106 (USA)

<sup>b</sup>Division of Biology, California Institute of Technology, 1200 E California Blvd, Pasadena, CA 91106 (USA)

### Abstract

Long-range communication is essential for the function of members of the Cys-loop family of neurotransmitter-gated ion channels. The involvement of the peptide backbone in binding-induced conformational changes that lead to channel gating in these membrane proteins is an interesting, but unresolved issue. To probe the role of the peptide backbone, we have incorporated a series of  $\alpha$ -hydroxy acid analogues into the  $\beta$ -sheet rich extracellular domain of the muscle subtype of the nicotinic acetylcholine receptor, the prototypical Cys-loop receptor. Specifically, mutations were made in  $\beta$ -strands 7 and 10 of the  $\alpha$ -subunit. A number of single backbone mutations in this region were well-tolerated. However, simultaneous introduction of two proximal backbone mutations led to surface-expressed, non-functional receptors. Together, these data suggest that while the receptor is remarkably robust in its ability to tolerate single amide-to-ester mutations throughout these  $\beta$ -strands, more substantial perturbations to this region have a profound effect on the protein. These results support a model in which backbone movements in the outer  $\beta$ -sheet are important for receptor function.

### Keywords

allosterism; backbone esters; ion channels; nicotinic receptor; unnatural mutagenesis

### Introduction

An essential feature of allsoteric proteins is that they are innately dynamic molecules, with the Cys-loop superfamily of ligand-gated ion channels providing a classic example. These neurotransmitter receptors are involved in mediating fast synaptic transmission throughout the central and peripheral nervous systems.[1–5] They are among the molecules of learning, memory, and sensory perception, and they are implicated in numerous neurological disorders, including Alzheimer's disease, Parkinson's disease, and schizophrenia. The muscle subtype of the nicotinic acetylcholine receptor (nAChR) is the prototypical Cys-loop receptor. It is a pentamer of homologous subunits arranged pseudo-symmetrically around a central ion-conducting pore. The extracellular domain is largely comprised of  $\beta$ -sheet structure and contains the agonist binding site. The agonist binding site itself is shaped by discontinuous flexible loop regions that meet at the interface between subunits. The primary contributors to the agonist binding site are in the  $\alpha$  subunit, with additional contributions from the complementary subunits ( $\gamma$  and  $\delta$ ). The transmembrane domain of each subunit is

made up of four membrane-spanning  $\alpha$ -helices, with one from each subunit lining the pore. Binding of a small molecule agonist in the extracellular domain triggers a series of conformational changes that leads to the opening of the channel gate some 60Å away.

Long-range communication is clearly critical in the function of these receptors.[6,7] Various models for how this communication occurs have been proposed, from specific side chain interactions to more rigid large-scale domain movements.[8–11] Recent linear free energy analysis of the nAChR has given rise to the notion of a “conformational wave”[8] that emanates from the agonist binding site to the gate of the channel in the transmembrane domain. It seems likely that some movement must occur in the immediate region of the binding interaction, with simple side chain movements comprising only a part of the ensuing conformational wave. Significant movements along the peptide backbone may also play a critical role in initiating channel gating.

To investigate the involvement of the peptide backbone in binding-induced conformational changes that lead to channel gating, we have incorporated a series of  $\alpha$ -hydroxy acid analogues into the  $\beta$ -sheet rich extracellular domain of the nAChR (Figure 1). Upon incorporation of an  $\alpha$ -hydroxy acid into a protein, the backbone amide functional group is replaced by an ester, with two major consequences (Figure 2). First, the ester bond disrupts the backbone hydrogen bonding pattern associated with  $\beta$ -sheet structure. The ester lacks the NH hydrogen bond donor, and the ester carbonyl is a weaker hydrogen bond acceptor than the amide carbonyl. Previous studies on a small 3-stranded  $\beta$ -sheet protein found that the effect of weakening a hydrogen bond acceptor (the carbonyl) is less destabilizing than removing the hydrogen bond donor (the NH) by about 0.8 kcal/mol.[12] Second, while the *s-trans* planar conformational preference, bond lengths, and bond angles are generally similar to those of amide bonds, the ester bond possesses much greater backbone flexibility due to substantial reduction of the rotation barrier around the C-O vs. the C-N single bond.

In the present work, amide-to-ester mutations were made in two critical  $\beta$ -strands that connect the agonist binding site to the transmembrane region of the receptor (Figure 1). To our knowledge, this is the first systematic study of amide-to-ester mutations in a  $\beta$ -sheet of a large allosteric receptor. Specifically, mutations were made in  $\beta$ -strands 7 and 10 ( $\beta$ 7 and  $\beta$ 10, respectively) of the  $\beta$ -subunit, disrupting the extensive backbone hydrogen bonding network in what has been termed the outer  $\beta$ -sheet of the extracellular domain. The rationale behind studying these strands was two-fold. First,  $\beta$ 7 connects the critical cation- $\pi$  binding residue in loop B ( $\alpha$ W149)[13] to the eponymous Cys-loop, which directly contacts the transmembrane region.  $\beta$ 10 extends from loop C, which contains two other aromatic binding box residues[14,15], and connects directly to the first transmembrane helix. Second, recent studies strongly implicate the outer  $\beta$ -sheet in connecting agonist binding to channel gating.[10,16–19] A study of  $\beta$ 7 and  $\beta$ 10 in the neuronal  $\alpha$ 7 nAChR suggests that the rigidity of this region is crucial in transducing channel gating.[17] Furthermore, previous studies show that a triad of residues in this region is important in initiating channel gating.[10] These residues are the C-loop residue  $\alpha$ Y190, along with  $\alpha$ K145 and  $\alpha$ D200, on  $\beta$ 7 and  $\beta$ 10, respectively. Thus, it seemed reasonable to assume that the outer  $\beta$ -sheet was important for connecting agonist binding to channel gating, and that backbone dynamics and hydrogen bonding might be involved. Given that the balance between rigidity and flexibility is believed to be central to the structure and function of allosteric proteins,[7] involvement of the peptide backbone in mediating allosteric communication in the nAChR would not be surprising. Previous studies of backbone esters in ion channels have focused on the role of backbone flexibility in  $\alpha$ -helical domains,[20–22] seeking local movements that directly influence channel gating. Here we hope to better understand how hydrogen bonding in a critical  $\beta$ -sheet region that is distal to the channel gate influences receptor function.

Surprisingly, a number of single backbone mutations in this region were well-tolerated, producing only modest shifts in  $EC_{50}$  and wild type-like macroscopic current sizes ( $I_{max}$ ) in the majority of cases. However, simultaneous introduction of two backbone mutations either in the same  $\beta$ -strand separated by a single amino acid or at amino acids sharing a hydrogen bond between the two  $\beta$ -strands led to surface-expressed, non-functional receptors. Together, these data suggest that while the receptor is remarkably robust in its ability to tolerate single amide-to-ester mutations throughout these  $\beta$ -strands, more substantial perturbations to this region have a profound effect on the protein. Therefore, it would seem that backbone movements in the outer  $\beta$ -sheet are important for receptor function. This adds to a growing body of evidence that points to the importance of this region in mediating the conformational changes that emanate from the agonist binding site to the gate of the channel.

## Results

### Single amide-to-ester mutations in $\beta 7$ and $\beta 10$ have minimal impact on receptor function

Nine  $\alpha$ -hydroxy acids were incorporated into  $\beta 7$  and  $\beta 10$  of the  $\alpha$ -subunit extracellular domain, perturbing a total of 13 hydrogen bonds (Figure 1). In some cases, the  $\alpha$ -hydroxy analogue of the native amino acid was not available. In these instances, conventional mutagenesis was employed to find an alternative amino acid side chain that had both minimal effect on receptor function and an available  $\alpha$ -hydroxy analogue. The effect of the amide-to-ester mutation was then compared to the analogous side chain mutant, instead of the wild-type receptor. Most amide-to-ester mutations produced modest changes in  $EC_{50}$  (< 2-fold) (Figure 3, Table 1). In three cases ( $\alpha M144$ ,  $\alpha L199$ , and  $\alpha V206$ ) larger, although still not immense, shifts in the 3.5-4-fold range were seen. ACh-induced whole-cell currents of receptors with single  $\alpha$ -hydroxy mutations were similar to the currents produced by incorporation of the native amino acid by nonsense suppression.

As  $EC_{50}$  is a composite of both binding and gating phenomena, small shifts in  $EC_{50}$  may mask a large effect on receptor behavior. Recently, we developed a method to evaluate whether a loss of function (increase in  $EC_{50}$ ) mutation in the extracellular domain strongly impacts receptor gating (rather than agonist binding).[23] The method, termed ELFCAR (Elucidating Long-range Functional Coupling in Allosteric Receptors), is based on mutant cycle analysis and produces a value for  $\Omega$ , the coupling between extracellular domain residue and a known gating mutation (in this case  $\beta L9'S$ ). This method utilizes whole-cell data to determine whether a mutant that produces a moderate to large increase in  $EC_{50}$  has a substantial impact on receptor gating, as indicated by  $\Omega > 2$ . ELFCAR is especially valuable in interpreting moderate increases in  $EC_{50}$ , where a dramatic effect on gating might otherwise be missed. An  $\Omega$  value near one, however, does not preclude a modest effect on gating. The three  $\alpha$ -hydroxy mutants in this study that produce increases in  $EC_{50}$  – at positions 144, 201, and 206 – all produce an  $\Omega$  value near one (0.97, 0.65, and 0.69, respectively), suggesting no dramatic impact on receptor gating. This method is not applicable to gain-of-function mutations, so the remaining six mutants could not be evaluated using ELFCAR. Combined, the data suggest that single  $\alpha$ -hydroxy mutations in this region do not substantially impair receptor gating.

### Simultaneous incorporation of two $\alpha$ -hydroxy acid mutations in $\beta 7$ and $\beta 10$ produces non-functional, surface expressed receptors

The impact of disrupting the polypeptide backbone at more than one location was investigated by simultaneously incorporating two  $\alpha$ -hydroxy acids. This was done in two different ways: amide-to-ester mutations were made either in the same  $\beta$ -strand separated by a single amino acid ( $\alpha M144$  and  $\alpha L146$  in  $\beta$ -strand 7), or at amino acids sharing a hydrogen

bond between the two  $\beta$ -strands ( $\alpha$ L146 and  $\alpha$ I201; Figure 1). Simultaneous incorporation of the same  $\alpha$ -hydroxy (Lah) or amino (Leu, in the case of wild type recovery) acid was done in both scenarios. This allowed for double suppression using the standard nonsense suppression methodology (see Materials and Methods). As a large shift in  $EC_{50}$  might have been anticipated, the double mutation experiments were carried out in the presence of the  $\beta$ L9'S gating mutation. For mutations that primarily affect binding or have a only moderate effect on channel gating this mutation lowers the  $EC_{50}$  by about 40-fold, allowing for reliable  $EC_{50}$  measurement of potentially highly deleterious mutations without complications from open channel block at high agonist concentrations.

For both double-mutation (Lah) experiments, no whole-cell current was observed in response to high (>1000  $\mu$ M) doses of ACh. Wild type recovery (Leu) by nonsense suppression gave normal whole cell currents in the range of 5 to 15  $\mu$ A. Lack of an electrophysiological response can indicate that protein folding, subunit assembly, receptor transport, or receptor function have been impacted.

To determine whether nonfunctional mutant receptors were expressed at the plasma membrane, the localization of these mutant receptors was studied using single molecule Total Internal Reflectance Fluorescence (TIRF) microscopy. Mutant and wild type (recovery by nonsense suppression) receptors were first labelled with biotin conjugated to  $\alpha$ -bungarotoxin and subsequently labelled with streptavidin conjugated to the fluorophore Alexa488. Fluorescent puncta corresponding to single receptors were clearly visible on the cell surface (Figure 4B). For the double  $\alpha$ -hydroxy-containing receptors, the number of puncta was between 50 and 70% of the value seen for wild type receptor (recovery by nonsense suppression) (Figure 4B, Table 2). Based on previous, extensive studies with this approach,[24] it is clear that double mutant receptors are being surface expressed at a level such that significant whole-cell current would be observed, if the receptors were functional. That is, the calculated expected whole-cell currents from the  $\alpha$ -hydroxy double mutant receptors based on puncta density are on the order of 3 to 5  $\mu$ A (Table 2). Since we can easily detect this magnitude of Ach-induced current, our results clearly show that non-functional receptors have been expressed on the oocyte surface. The calculated expected whole cell currents from the wild type receptors based on puncta density are on the order of 6 to 7  $\mu$ A, in agreement with the electrophysiological data.

Note that  $\alpha$ -bungarotoxin is a potent inhibitor of the nAChR that binds tightly in the same region[25] as ACh and requires properly folded receptor for tight binding. Thus, successful  $\alpha$ -bungarotoxin binding indicates that the overall structure of the extracellular domain and binding site were not grossly perturbed. These results indicate that simultaneous incorporation of two  $\alpha$ -hydroxy mutations in this region leads to nonfunctional, surface-expressed receptors.

## Discussion

The  $\beta$ -sandwich structure comprised of “inner” and “outer”  $\beta$ -sheets – first revealed in the AChBP structure[14,15] and later confirmed in images of the full nAChR[18,26] – is accepted to be a critical structural feature of Cys-loop receptors. In the present work, we have probed the robustness of this structure by selectively removing/weakening backbone hydrogen bonds that define the structure, using backbone ester substitution. The remarkable generality of nonsense suppression techniques for incorporating unnatural residues into receptors and channels expressed in *Xenopus* oocytes makes this study possible. One could have imagined several outcomes for such experiments. If movement within the sheets is critical to receptor function, backbone mutations could facilitate receptor gating, perhaps

even creating constitutively active receptors. Alternatively, if an intact  $\beta$ -sandwich is essential for receptor function, backbone mutations could disable the receptor.

Here we have focused on the outer  $\beta$ -sheet of the extracellular domain, and in particular on  $\beta 7$  and  $\beta 10$ , which have been proposed to play key roles in receptor function. Perhaps surprisingly, individual amide-to-ester mutations throughout both strands resulted in functional receptors with only modest changes in  $EC_{50}$ . Evidently, the outer  $\beta$ -sheet is relatively robust, and the receptor can absorb the loss of a single hydrogen bond in this region. Interestingly, however, simultaneous replacement of two nearby residues with their  $\alpha$ -hydroxy analogues produced surface-expressed, but non-functional receptors. Using receptor labelling with fluorescent  $\alpha$ -bungarotoxin, and single-molecule imaging by TIRF microscopy, we demonstrate that the number of double-mutant receptors expressed on the oocyte is more than adequate to produce measurable currents, if the receptors were functional. Tight binding by  $\alpha$ -bungarotoxin requires proper folding in the region of the agonist binding site, which is quite near the mutations considered here. In fact, in the  $\alpha$ -bungarotoxin-bound crystal structure of the  $\alpha 1$ -subunit,[27] residues at the top of both  $\beta 7$  and  $\beta 10$  are in close proximity to the bound  $\alpha$ -bungarotoxin molecule. Successful binding of  $\alpha$ -bungarotoxin to the double mutant receptors, as detected by TIRF microscopy, strongly suggests that the structure of this region is not greatly perturbed.

The implication is that the crucial outer  $\beta$ -sheet of the nAChR is not overly fragile – it can tolerate the disruption caused by a single backbone substitution – but it must be intact for receptor function, and apparently two proximal backbone mutations are too disruptive. Folding, assembly, and transport to the cell surface, however, can still occur in the double mutants discussed here.

These results can be understood in the context of emerging models of the conformational changes in the extracellular domain that lead to receptor activation. Recent MD simulations[19,28] have pointed to a pivotal role for  $\beta 10$  in communicating the inward motion of the agonist binding site-shaping C-loop to the motions of the transmembrane domain that eventually produce channel opening. The proposed upward and outward motion allows  $\alpha R209$  on  $\beta 10$  to approach  $\alpha E45$  on the  $\beta 2$ – $\beta 3$  linker, resulting in an interaction between these two residues; an interaction that was previously concluded to be important for coupling agonist binding and channel gating based on mutant cycle analysis of single channel data.

$\beta 7$  likewise harbors a residue,  $\alpha K145$ , that has been implicated in connecting agonist binding with channel gating. When agonist binds and the C-loop closes in, a salt bridge between  $\alpha K145$  on  $\beta 7$  and  $\alpha D200$  on  $\beta 10$  breaks, and  $\alpha K145$  forms a hydrogen bond with  $\alpha Y190$  on the C-loop.[10] This electrostatic rearrangement was proposed to initiate conformational changes that contribute to opening of the central ion-conducting pore.

Studies of engineered disulfide linkages between  $\beta 7$  and  $\beta 10$  in the  $\alpha 7$  nAChR also suggest that the outer  $\beta$ -sheet plays a role in transmitting agonist binding-induced conformational changes to the channel gate.[17] Specifically, in the background of a non-desensitizing mutation, one engineered disulfide-containing receptor could be activated by divalent cations alone, which normally play a role as allosteric modulators. This implies that reduced mobility in the outer  $\beta$ -sheet of these receptors results in a lower barrier to channel activation. These and other researchers[16] have suggested that this  $\beta$ -sheet may act as a lever, where binding at one end tilts the lever resulting in a movement at the other, transmembrane-adjacent, end. A certain amount of rigidity in this region seems to be fundamental to normal receptor function.

Using this lever analogy, our results suggest that two or more nearby  $\alpha$ -hydroxy acid mutations lead to a more flexible and thus ineffective lever that is unable to communicate agonist binding events to the transmembrane region of the receptor. Thus, disruption of hydrogen bonding in the outer  $\beta$ -sheet would seem to interrupt the conformational wave that connects the agonist binding-induced motions of the C-loop to the subsequent motions of the transmembrane region.

It is also possible that the loss of hydrogen bonding between these strands could lead to misalignment of the binding box residues, impairing agonist binding to the receptor. However, it seems less likely that the binding region of the receptor is grossly malformed, since  $\alpha$ -bungarotoxin is still able to bind to the mutant receptors.

## Conclusion

In conclusion, we find that the network of hydrogen bonds formed in the outer  $\beta$ -sheet of the nAChR is fairly robust, tolerating single amide-to-ester mutations throughout. However, eliminating two proximal hydrogen bonds completely destroys receptor function, adding further support to gating models that ascribe important roles to these  $\beta$ -strands of the nAChR extracellular domain.

## Experimental Section

### Unnatural Hydroxy Acid Suppression

Synthetic  $\alpha$ -hydroxy acids were conjugated to the dinucleotide dCA and ligated to truncated 74-nucleotide tRNA as previously described.[29] Typically, 25 ng of tRNA was injected per oocyte along with mRNA in a total volume of 50 nL/cell. mRNA was prepared by in vitro runoff transcription using the Ambion (Austin, TX) T7 mMessage mMachine kit. The site of interest was mutated to the amber stop codon by standard means, verified by sequencing through both strands. Mouse muscle embryonic nAChR in the pAMV vector was used. A total of 4.0 ng of mRNA was injected in an  $\alpha$ : $\beta$ : $\gamma$ : $\delta$  subunit ratio of 10:1:1:1. The ratio of tRNA to mRNA was typically 1:1. In addition, the  $\alpha$ -subunits contain an HA epitope in the M3–M4 cytoplasmic loop for Western blot studies. Control experiments show that this epitope does not detectably alter EC<sub>50</sub>. As a negative control for suppression, truncated 74-nucleotide tRNA or truncated tRNA ligated to dCA to give a 76mer was co-injected with mRNA in the same manner as fully charged tRNA. Data from experiments where currents from these negative controls was greater than 10% of the experimental were excluded. The positive control for suppression involved wild-type recovery by co-injection with 74-nucleotide tRNA ligated to wild type amino acid. For suppression at multiple sites, the tRNA:mRNA ratio was increased to 2:1.

### Electrophysiology

Stage V–VI oocytes of *Xenopus laevis* were employed. Oocyte recordings were made 12–48 h post injection in two-electrode voltage clamp mode using the OpusXpress 6000A instrument (Axon Instruments, Union City, CA). Oocytes were superfused with a Ca<sup>2+</sup>-free ND96 solution at flow rates of 1 mL/min before application, (15 second) 4 mL/min during drug application, and 3 mL/min during wash. Holding potentials were –60 mV. Data were sampled at 125 Hz and filtered at 50 Hz. Acetylcholine chloride was purchased from Sigma/Aldrich/RBI. Solutions ranging from 0.01 mM to 5000 mM were prepared in Ca<sup>2+</sup>-free ND96 from a 1 M stock solution. Dose-response data were obtained for a minimum of 8 concentrations of agonists and for a minimum of five cells. Dose-response relations were fitted to the Hill equation to determine EC<sub>50</sub> and Hill coefficient values. The dose-response relations of individual oocytes were examined and used to determine outliers. The reported EC<sub>50</sub> values are from the curve fit of the averaged data.

## Total Internal Reflection Fluorescence Microscopy

*Xenopus* oocytes were prepared for single molecule TIRF microscopy as follows. 24–48 hours after injection of mRNA and tRNA, oocytes were incubated in a 0.5 ng/μL solution of biotin conjugated to  $\alpha$ -bungarotoxin (Molecular Probes, Invitrogen, Eugene, OR) for 4–12 hours. This was followed by two wash steps with a 5 mg/mL bovine serum albumin solution and one wash with  $\text{Ca}^{2+}$ -free ND96. Subsequently, oocytes were incubated in a 0.2 ng/μL solution streptavidin conjugated to the fluorophore Alexa488 (Molecular Probes, Invitrogen, Eugene, OR) for 15–30 minutes, followed by two additional wash steps each with BSA and  $\text{Ca}^{2+}$ -free ND96. The vitelline membrane of labeled oocytes was removed with forceps following a 5–10 minute incubation in a hypertonic solution (220 mM sodium aspartate, 10 mM HEPES, 10 mM EDTA, 2 mM  $\text{MgCl}_2$ , pH 7.38). Devitellinized oocytes were transferred to an imaging chamber with a clean glass coverslip mounted on the microscope stage with the animal pole oriented toward the coverslip. The TIRF microscope used to collect the data consists of a Melles-Griot Argon (Ar) ion laser coupled to a fiber optic which extends to an Olympus TIRF illuminator adapted to a standard inverted IX-71 Olympus microscope (Center Valley, PA). A wavelength of 488 nm was used to excite and detect the Alexa488 fluorophores, by using the Z488 filter cube from Chroma Technology Corporation (Rockingham, VT). A 100 $\times$  1.45 NA Olympus TIRF objective was used. Images were captured with a Photometrics Cascade front illuminated CCD camera from Princeton Instruments (Trenton, NJ). Andor iQ from Andor Technology (South Windsor, CT) was used to acquire the data. The data were subsequently processed and analyzed with ImageJ (National Institutes of Health). Puncta were manually counted and densities from  $\geq 6$  images and  $\geq 2$  oocytes were compiled and averaged. Expected current sizes were calculated as (#puncta/image frame area)\*average oocyte area\*single channel conductance.

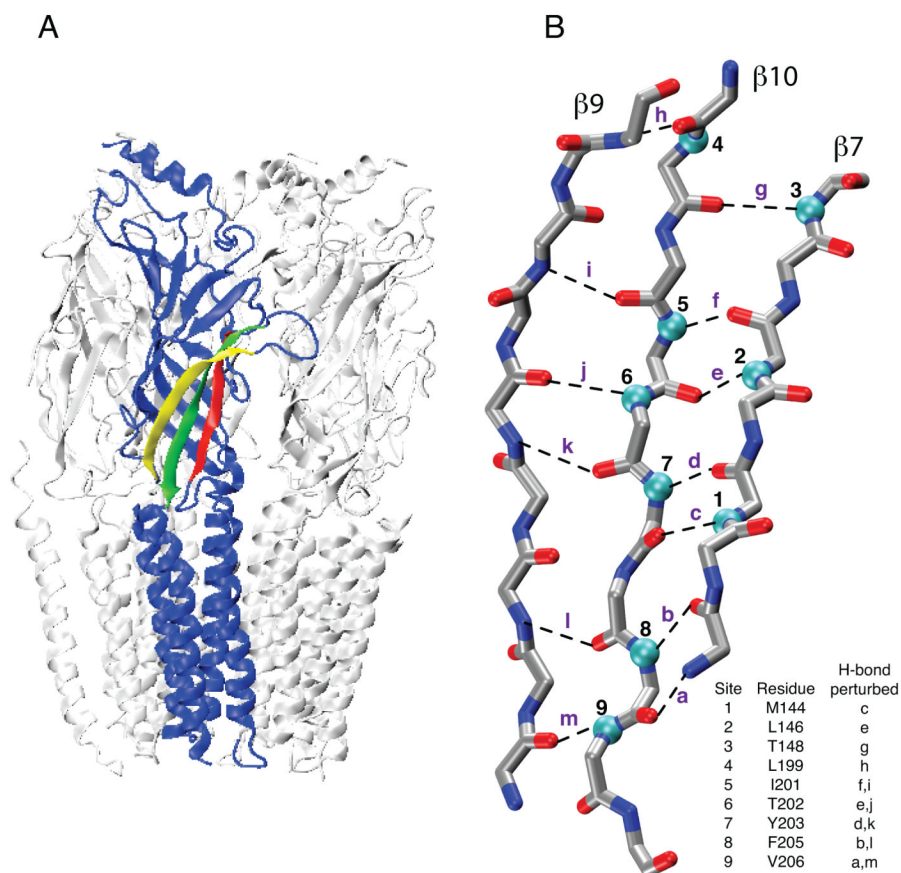
## Acknowledgments

We thank Dr. Rigo Pantoja for advice and assistance with TIRF measurements. This work was supported by the NIH (NS 34407; NS 11756). K. R. G. was partially supported by an NSF Graduate Research Fellowship.

## References

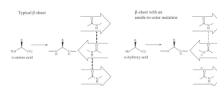
1. Corringer PJ, Le Novère N, Changeux JP. *Annu Rev Pharmacol Toxicol.* 2000; 40:431. [PubMed: 10836143]
2. Grutter T, Changeux JP. *Trends Biochem Sci.* 2001; 26:459. [PubMed: 11504610]
3. Connolly CN, Wafford KA. *Biochemical Society Transactions.* 2004; 32:529. [PubMed: 15157178]
4. Lester HA, Dibas MI, Dahan DS, Leite JF, Dougherty DA. *Trends in Neurosciences.* 2004; 27:329. [PubMed: 15165737]
5. Sine SM, Engel AG. *Nature.* 2006; 440:448. [PubMed: 16554804]
6. Changeux JP, Edelstein SJ. *Science.* 2005; 308:1424. [PubMed: 15933191]
7. Cui Q, Karplus M. *Protein Sci.* 2008; 17:1295. [PubMed: 18560010]
8. Grosman C, Zhou M, Auerbach A. *Nature.* 2000; 403:773. [PubMed: 10693806]
9. Lee WY, Sine SM. *Nature.* 2005; 438:243. [PubMed: 16281039]
10. Mukhtasimova N, Free C, Sine SM. *J Gen Physiol.* 2005; 126:23. [PubMed: 15955875]
11. Xiu X, Hanek AP, Wang J, Lester HA, Dougherty DA. *J Biol Chem.* 2005; 280:41655. [PubMed: 16216879]
12. Deechongkit S, Dawson PE, Kelly JW. *J Am Chem Soc.* 2004; 126:16762. [PubMed: 15612714]
13. Zhong W, Gallivan JP, Zhang Y, Li L, Lester HA, Dougherty DA. *Proc Natl Acad Sci U S A.* 1998; 95:12088. [PubMed: 9770444]
14. Brejc K, van Dijk WJ, Klaassen RV, Schuurmans M, van Der Oost J, Smit AB, Sixma TK. *Nature.* 2001; 411:269. [PubMed: 11357122]
15. Sixma TK, Smit AB. *Annu Rev Biophys Biomol Struct.* 2003; 32:311. [PubMed: 12695308]

16. Law RJ, Henschman RH, McCammon JA. *Proc Natl Acad Sci U S A*. 2005; 102:6813. [PubMed: 15857954]
17. McLaughlin JT, Fu J, Sproul AD, Rosenberg RL. *Mol Pharmacol*. 2006; 70:16. [PubMed: 16533908]
18. Unwin N. *Journal of Molecular Biology*. 2005; 346:967. [PubMed: 15701510]
19. Yi M, Tjong H, Zhou HX. *Proc Natl Acad Sci U S A*. 2008; 105:8280. [PubMed: 18541920]
20. England PM, Zhang Y, Dougherty DA, Lester HA. *Cell*. 1999; 96:89. [PubMed: 9989500]
21. Lu T, Ting AY, Mainland J, Jan LY, Schultz PG, Yang J. *Nat Neurosci*. 2001; 4:239. [PubMed: 11224539]
22. Nagaoka Y, Shang L, Banerjee A, Bayley H, Tucker SJ. *Chembiochem*. 2008; 9:1725. [PubMed: 18543260]
23. Gleitsman KR, Shanata JAP, Frazier SJ, Lester HA, Dougherty DA. *Biophys. J*. 2009 in press.
24. Pantoja R, Rodriguez EA, Dibas MI, Dougherty DA, Lester HA. *Biophys J*. 2009; 96:226. [PubMed: 19134478]
25. Nirthanan S, Gwee MC. *J Pharmacol Sci*. 2004; 94:1. [PubMed: 14745112]
26. Miyazawa A, Fujiyoshi Y, Unwin N. *Nature*. 2003; 423:949. [PubMed: 12827192]
27. Dellisanti CD, Yao Y, Stroud JC, Wang ZZ, Chen L. *Nat Neurosci*. 2007; 10:953. [PubMed: 17643119]
28. Cheng X, Wang H, Grant B, Sine SM, McCammon JA. *PLoS Comput Biol*. 2006; 2:e134. [PubMed: 17009865]
29. Nowak MW, Gallivan JP, Silverman SK, Labarca CG, Dougherty DA, Lester HA. *Methods Enzymol*. 1998; 293:504. [PubMed: 9711626]

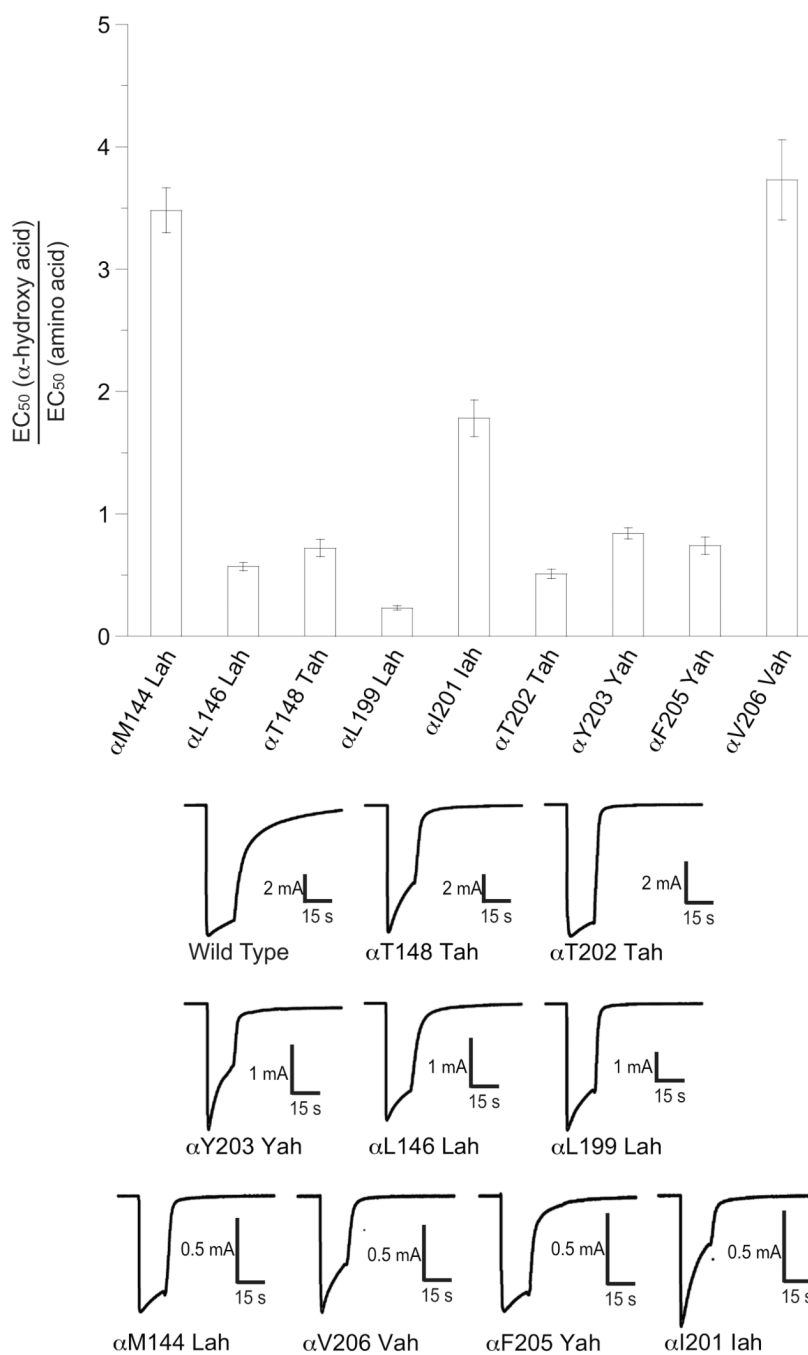


**Figure 1.**

Two views of the nAChR. (A) Overall layout of the receptor. One of the five subunits is shown in blue, with  $\beta 7$ ,  $\beta 9$ , and  $\beta 10$  highlighted in red, yellow, and green, respectively. (B) The hydrogen bonding network of the outer  $\beta$ -sheet of the nAChR. Turquoise balls indicate positions at which the backbone NH was mutated to an oxygen. The black dashed lines indicate hydrogen bonds that are completely removed or attenuated due as a result of mutation. Image is based cryo-EM of the full *Torpedo* receptor (2bg9).[18]

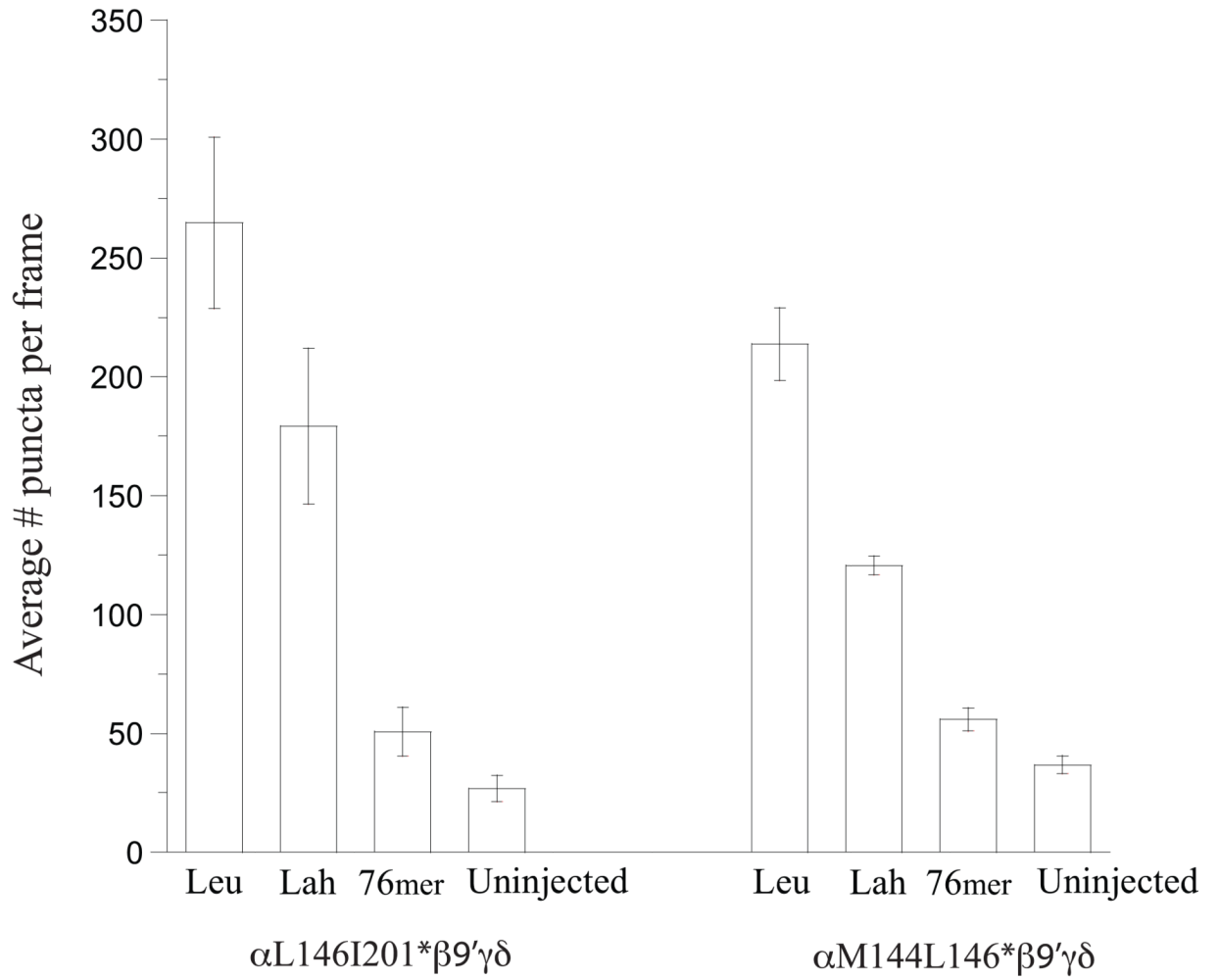


**Figure 2.** Schematic of the backbone amide versus the backbone ester bond in the context of a  $\beta$ -sheet.



**Figure 3.** Characteristics of nAChR with backbone mutations in  $\beta$ -strands 7 and 10. (A) EC<sub>50</sub> shifts for backbone mutations made at nine positions in  $\beta$ 7 and  $\beta$ 10. Modest effects on receptor function are seen in all cases. (B) Current traces for backbone mutations made at nine positions in  $\beta$ 7 and  $\beta$ 10.

## 4A



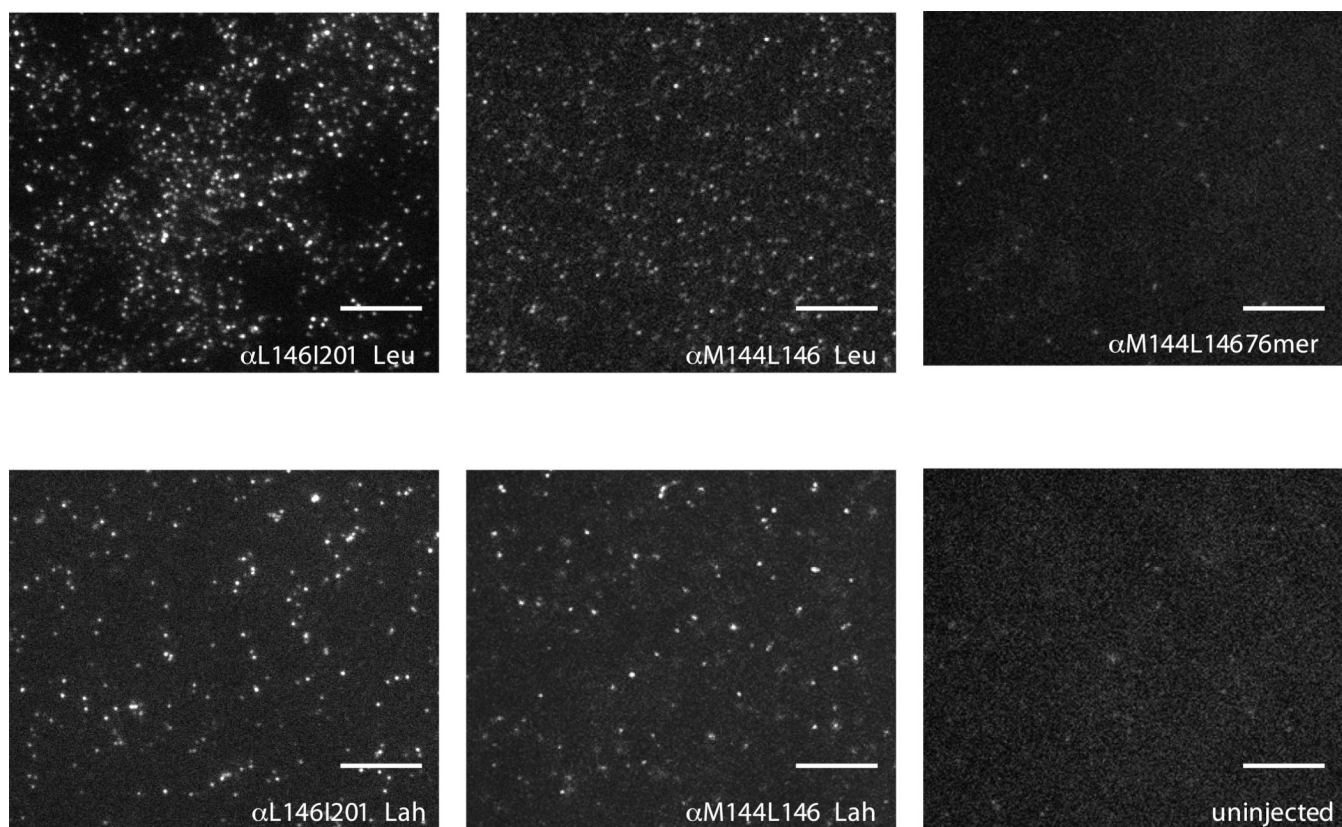


**Figure 4.** Analysis of non-functional nAChRs containing two amide-to-ester mutations by TIRF microscopy. (A) Puncta density for receptors labeled with Leu refers to recovery of the wild-type peptide backbone by nonsense suppression; Lah refers to incorporation of leucine  $\alpha$ -hydroxy; and 76mer indicates the negative control experiment (coinjection of mRNA with a tRNA molecule that has not been charged with an amino or hydroxy acid). The puncta density for both Leu and Lah are significantly higher than for either the 76mer or uninjected oocyte controls (t-test values for Lah vs. 76mer are:  $P=0.0009$  (L146I120);  $P<0.0001$  (L146M144); for Lah vs. uninjected:  $P=0.0003$  (L146I120);  $P<0.0001$  (L146M144). Data are compiled from  $\geq 6$  non-overlapping images from  $\geq 2$  oocytes. (B) Representative TIRF images corresponding to the data in (A). Scale bars represent  $6\ \mu\text{m}$ .

**Table 1**

EC<sub>50</sub> and Hill coefficient ( $\pm$ SEM) values for mutations made in this study.

	EC <sub>50</sub> ( $\mu$ M)	n <sub>H</sub>
WT	46 $\pm$ 2	1.8 $\pm$ 0.13
$\alpha$ M144Leu	15 $\pm$ 0.3	1.7 $\pm$ 0.06
$\alpha$ M144Lah	50 $\pm$ 0.8	1.7 $\pm$ 0.03
$\alpha$ L146Lah	26 $\pm$ 0.8	1.3 $\pm$ 0.05
$\alpha$ T148Tah	33 $\pm$ 3	1.0 $\pm$ 0.06
$\alpha$ L199Lah	11 $\pm$ 0.5	1.6 $\pm$ 0.10
$\alpha$ I201Iah	82 $\pm$ 6	1.5 $\pm$ 0.12
$\alpha$ T202Tah	24 $\pm$ 1	1.4 $\pm$ 0.09
$\alpha$ Y203Yah	39 $\pm$ 0.8	1.9 $\pm$ 0.07
$\alpha$ F205Tyr	90 $\pm$ 2	1.5 $\pm$ 0.05
$\alpha$ F205Yah	67 $\pm$ 62	1.4 $\pm$ 0.13
$\alpha$ V206Vah	170 $\pm$ 10	1.9 $\pm$ 0.20

**Table 2**

Puncta densities and corresponding estimated current sizes from TIRF microscopy experiments. 76mer refers to unaminoacylated tRNA.

$\alpha$ I201L146	# Puncta/ image frame	Calculated current size ( $\mu$ A)
Leu	265 $\pm$ 36	7.5 $\pm$ 1.0
Lah	179 $\pm$ 33	5.1 $\pm$ 0.9
76mer	51 $\pm$ 10	1.4 $\pm$ 0.3
Uninjected	27 $\pm$ 5	0.8 $\pm$ 0.2
<hr/>		
$\alpha$ L146M144		
<hr/>		
Leu	214 $\pm$ 15	6.1 $\pm$ 0.4
Lah	121 $\pm$ 4	3.4 $\pm$ 0.1
76mer	56 $\pm$ 5	1.6 $\pm$ 0.1
Uninjected	37 $\pm$ 4	1.0 $\pm$ 0.1